Available online at www.sciencedirect.com
ScienceDirect
ELSEVIER
International Journal of Mass Spectrometry 261 (2007) 91–99
International Journal of Mass Spectrometry
www.elsevier.com/locate/ijms

A TRIDYN study: Comparison of experimental SIMS useful yields with simulated Cs concentration evolution

P. Philipp [a,*], T. Wirtz [a], H.-N. Migeon [a], H. Scherrer [b]

[a] *Département Science et Analyse des Matériaux, Centre de Recherche Public – Gabriel Lippmann, 41 rue du Brill, L-4422 Belvaux, Luxembourg*
[b] *Laboratoire de Physique des Matériaux, Ecole des Mines, Parc de Saurupt, F-54042 Nancy Cedex, France*

Received 13 June 2006; received in revised form 27 July 2006; accepted 28 July 2006
Available online 15 September 2006

Abstract

In a previous paper by the same authors, the sensitivity variations of negative secondary ions during Secondary Ion Mass Spectrometry (SIMS) analysis have been studied with respect to conditions of neutral cesium deposition. An experimental determination of the Cs surface concentration was impossible and it has been described by characteristic parameters. In this paper, the TRIDYN model is used to simulate these surface concentrations with respect to the different conditions used in the experimental study. The simulations give implantation profiles as well as sputtering yields of the involved elements with respect to the primary ion fluence. For the different experimental conditions, the implantation profiles at steady state are used to calculate mean Cs surface concentrations that have been averaged over different depths. The sensitivities of negative secondary ions can now be plotted with respect to these concentrations and experimental and simulated results can be compared to the electron-tunneling model describing ion emission from metallic and semi-conducting samples. Nevertheless, approximations included in this simulation model induce some artefacts which are discussed in this paper.
© 2006 Elsevier B.V. All rights reserved.

Keywords: TRIDYN; Neutral cesium deposition; Cesium surface concentration; Useful yield; Secondary Ion Mass Spectrometry

1. Introduction

Secondary Ion Mass Spectrometry (SIMS) represents a powerful surface and thin film analysis technique, due in particular to its excellent sensitivity, its high dynamic range and its good depth resolution [1,2]. It is widely used for analysis of trace elements in solid materials like semiconductors and thin films [1–3]. Emerging fields of applications for SIMS are biology and medicine in particular [4–6].

At the same time, the SIMS technique is complicated by the lack of quantification due to the matrix effect [7]: the ionization probability of secondary ions and thus the sensitivity of the analysis depends on the sample composition. In fact, the emission of secondary ions is very sensitive to the chemical state of the sample surface [3,7,8]. In particular, deposition and incorporation of electropositive elements produce drastically increased negative secondary ion yields on most surfaces. This increase of the analysis sensitivity can cover several orders of magnitude [9]. It has been shown that the deposition or incorporation of alkali metals (in particular cesium) decreases the electron work function of the sample [10–14] which induces an increase of the negative secondary ion sensitivity [15,16]. So the negative secondary ion yields strongly depend on the stationary Cs surface concentration [9,15,17–19].

Because of the abovementioned reasons, Cs^+ primary ion bombardment is widely used in SIMS analyses to effect this negative ion yield enhancement, thus providing higher detection sensitivities. On commercial dynamic SIMS instruments, this bombardment serves both for the incorporation of Cs in the sample and for the sputtering of the surface. In such conditions, the primary ion bombardment conditions (mainly impact energy and incidence angle, which can be adapted only in a very limited way on conventional SIMS equipment) as well as the characteristics of the investigated sample imply a distinct total sputtering yield, and consequently determine the Cs surface concentration. In consequent, the Cs surface concentration is almost fixed for a given type of sample and an optimization of the secondary ion yield is impossible. Up to now, studies examining the effect of Cs surface concentration on negative secondary ion sensitivities were mainly limited to the Cs surface concentration evolution

* Corresponding author. Tel.: +352 47 02 61 559; fax: +352 47 02 64.
E-mail address: philipp@lippmann.lu (P. Philipp).

1387-3806/$ – see front matter © 2006 Elsevier B.V. All rights reserved.
doi:10.1016/j.ijms.2006.07.020

in the transient regime or to the Cs concentration obtained by different bombardment conditions [15,19].

The Cation Mass Spectrometer (CMS), which is a SIMS prototype developed in our laboratory, has been designed to overcome this problem [20–25]. This instrument is equipped with a patented neutral Cs° evaporator [26] to vary the Cs surface concentration over the whole range and to ensure in that way an optimal Cs concentration for maximum negative secondary ion sensitivities. In such experimental conditions, the adjustment of the Cs surface concentration is decoupled from primary bombardment and the primary ion type can be chosen with respect to the application. A detailed study on the evolution of negative secondary ion sensitivities with respect to the Cs deposition conditions has been presented in a previous paper [27]. During this study, the Cs concentration could not be determined but only represented by a characteristic parameter.

Compared to other similar techniques with quantification possibilities like SIMS in the MCs^+ technique or Secondary Neutral Mass Spectrometry (SNMS), the main advantage of M^- SIMS using cesium deposition combined with simultaneous primary ion bombardment is the significantly higher analysis sensitivity leading to detection limits down to the ppb range. For SNMS [28–30] or the MCs^+ technique [23,24], the detection limits are limited to the ppm range. Only laser SNMS shows similar detection limits than SIMS with Cs° deposition but quantification is problematic.

This paper is meant to simulate the Cs surface concentration for the experimental conditions used in the aforementioned study [27] in order to compare the experimental results to the model used to describe ion emission from metallic and semi-conducting surfaces. For this purpose the simulation code TRIDYN is used [31–33]. The TRIDYN code is based on TRIM [34–36], which simulates ion irradiation of amorphous targets in the binary collision approximation by using the Monte Carlo method. So thermal dependent processes like diffusion and segregation are ignored. While TRIM allows only the simulation of a pure static system (each ion impact happens on a non-irradiated target), TRIDYN simulates the evolution of the system with the primary ion fluence giving access to the system composition and sputtering parameters in the equilibrium regime. The comparison between simulation and experimental results will be performed in this steady state. For this study it is especially useful to reproduce the Cs concentration with respect to the ion and neutral cesium fluence and to get hold of this concentration in the equilibrium regime.

As the TRIDYN code uses the Monte Carlo method, the Cs surface concentration and all the other results calculated by the simulations are only semi-quantitative. But in order to compare the experimental useful yields to the theoretical model, quantitative data is not necessary. Only the relative variations of the Cs surface concentration with respect to the different experimental conditions are important for this comparison.

2. Experimental

The simulation conditions are chosen identical to the experimental conditions used in the previous study [27]. Primary ion bombardment and neutral Cs deposition are simultaneously applied on different targets. Primary ion bombardment is performed using Ga^+ and Cs^+ ions. Ga^+ bombardment is carried out with an impact energy of 32.5 keV and an incidence angle of 40° while Cs^+ bombardment is performed with an impact energy of 13.0 keV and an incidence angle of 35°. Cs atoms are deposited with an energy of 0 eV and an incidence angle of 45°. Ga^+ bombardment with simultaneous metallic Cs deposition will be denoted by Ga^+/Cs° bombardment and Cs^+ bombardment with simultaneous neutral Cs deposition will be denoted by Cs^+/Cs° bombardment.

Targets covering a considerable range on the work function scale and allowing the comparison of simple and binary compounds had been chosen in the previous study: Si, Al, Ni, InP and GaAs [27]. The same targets are used for the simulations.

The primary ion-neutral Cs fluence has been set to 10^{17} atoms/cm^2 for low Cs deposition rates (low fraction of Cs in incident beam of particles) and has been increased up to 8×10^{17} atoms/cm^2 for high Cs deposition rates (high fraction of Cs in incident beam of particles) in order to reach the equilibrium region for each simulation. The surface binding energy of each component was chosen equal to the heat of sublimation and independent of the target composition [37].

3. Results

The simulations are performed with respect to the parameters characterizing the Cs surface concentration in the previous study. For Ga^+/Cs° bombardment, the Cs surface concentration is characterized by the parameter τ which depends only on analytical parameters that can be determined easily [26,27]:

$$\tau = \frac{v_{\text{erosion}}}{v_{\text{deposition}}} \quad (1)$$

where v_{erosion} is the erosion velocity and $v_{\text{deposition}}$ is the Cs° deposition velocity.

For Cs^+/Cs° bombardment, we define analogously to relation (1) the characteristic parameter T [27]:

$$T = \frac{v_{\text{erosion}}}{v_{\text{deposition}}} \quad (2)$$

These parameters have been determined experimentally for different experimental conditions [27]. For a given value of τ or T, the simulation conditions will be taken identical to the experimental.

3.1. Simulations for Ga^+/Cs° bombardment

Only the results for Ga^+/Cs° bombardment on Si will be presented in detail. The results obtained on other samples show a similar behaviour. Fig. 1 shows implantation profiles in the equilibrium regime of Ga^+, Cs° and Si for different values of τ (53.9, 10.3, 1.3 and 0.2) obtained by Ga^+/Cs° bombardment on Si. In Fig. 1 the sign $^+$ indicates the primary ion, the sign $^{\circ}$ neutral Cs deposited at the sample surface and no sign is used for the elements of the sample. Simulations for τ equal to 53.9 and 10.3 use a fluence of 10^{17} atoms/cm^2. For τ equal to 1.3 a fluence of

Fig. 1. Depth profiles of Ga^+, Cs° and Si for Ga^+/Cs° bombardment on Si: (a) $\tau = 53.9$, (b) $\tau = 10.3$, (c) $\tau = 1.3$ and (d) $\tau = 0.2$.

2×10^{17} atoms/cm^2 was used and for τ equal to 0.2 the fluence was 4×10^{17} atoms/cm^2.

In Fig. 1, the concentration of Cs for all the values of τ is highest at the sample surface. For the different values of τ, the maximum Cs atomic fractions lie between 10^{-3} and 5×10^{-1}. Over the first few angstroms, the Cs concentration decreases over an order of magnitude, indicating that only a small fraction of the deposited Cs atoms are implanted by the Ga^+ bombardment into the sample. The steep decrease of the Cs concentration with respect to the depth is shown in Fig. 2 for τ equal to 1.3. For higher depths the concentration is close to 0. What's more, when comparing the maximum Cs concentration for the different values of the fluence in Fig. 2, important fluctuations of this concentration can be seen. They are probably due to the relatively small Cs concentration.

The Ga concentration at the sample surface is not influenced by the parameter τ (Fig. 1). It is mainly the Si surface concentration that decreases for higher values of τ, i.e., for higher Cs deposition velocities.

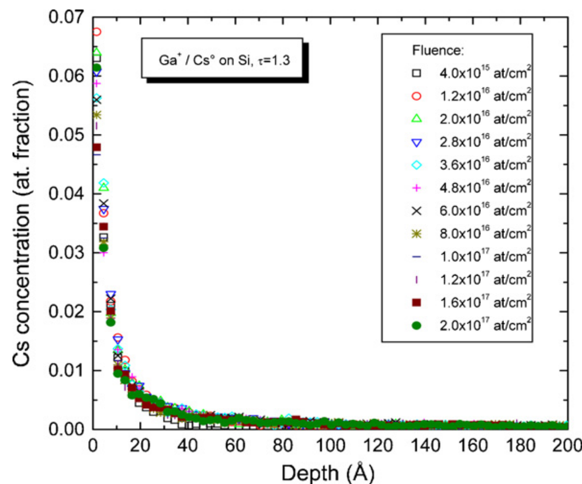

Fig. 2. Cs concentration with respect to the depth for $\tau = 1.3$ (Ga^+/Cs° bombardment on Si). The fluence is varying between 4.0×10^{15} and 2.0×10^{17} atoms/cm^2.

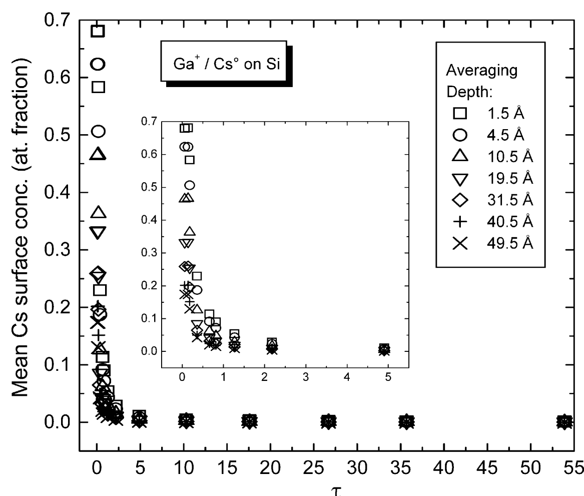

Fig. 3. Mean Cs surface concentration with respect to τ calculated by averaging the concentration evolution over depths varying from 1.5 to 49.5 Å (Ga^+/Cs° bombardment on Si).

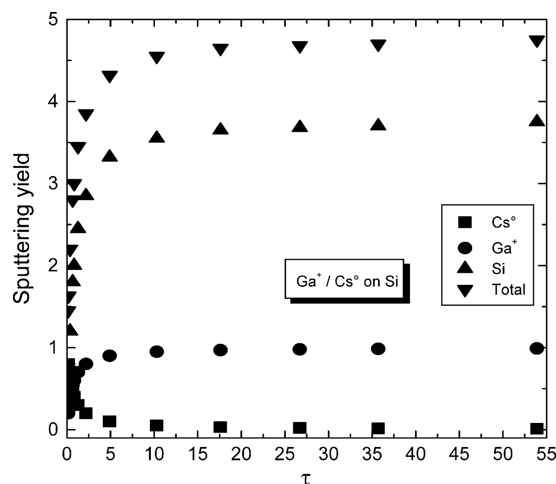

Fig. 4. Partial sputtering yields of Cs°, Ga^+ and Si and total sputtering yield with respect to τ for Ga^+/Cs° bombardment on Si.

In order to compare the simulation results to the previous experimental study [27], the Cs surface concentrations (in the equilibrium regime) must be extracted from the implantation profiles for the different values of τ. Therefore, mean surface concentrations averaged over a certain number of different depths have been calculated and plotted with respect to parameter τ (Fig. 3). The depths indicated in the caption of the graph correspond to the maximum depth over which the concentrations have been averaged. At low values of τ, the mean Cs surface concentration decreases very fast with respect to τ. For higher values of τ, the Cs surface concentrations are close to zero. Besides, for high values of τ the total amount of deposited Cs are low, implying that the mean Cs surface concentration is almost not dependent on the depth over which the concentrations have been averaged. For values of τ smaller than 2, the influence of the averaging depth on the mean surface concentrations increases. The concentration averaged over a depth of 1.5 Å is three times larger than the concentration averaged over 49.5 Å. As the Cs atoms deposited on the sample surface contribute most to the decrease of the sample work function [10–14] and the Cs surface concentration is highest for an averaging depth equal to 1.5 Å, the concentrations obtained at 1.5 Å are used in order to compare the experimental results to the electron-tunneling model [27].

The variation of the sputtering yield with respect to the parameter τ is also of interest for analyses realized with ion bombardment and simultaneous metallic Cs deposition (Fig. 4). As well as the partial sputtering yields of Si and Ga^+ as the total sputtering yield are highest for important values of τ (where the erosion rate is highest). For small values of τ, the amount of deposited Cs atoms compared to the number of incident Ga^+ ions increases, leading to an enlarged amount of Cs atoms to be sputtered and to reduced erosion rates. This explains the decreasing total sputtering yield as well as partial sputtering yields for Si and Ga^+.

Simulation results obtained for Ga^+/Cs° bombardment on Al and InP show a similar behaviour than those presented for Si. So only the mean Cs surface concentrations averaged over a depth of 1.5 Å have been plotted in Fig. 5. Compared to Al, the Cs concentration on InP is slightly higher for the high value of τ and begins to increase steeply for τ smaller than 15 whereas this sudden increase on Al is only observed for τ smaller than 5. So Al behaves similarly to Si. This difference between InP and Si or Al is due to the different masses. Al (26.9 amu) and Si (28.1 amu) have a similar mass whereas the mass of P (30.9 amu) is slightly higher and for In (114.8 amu) even much higher. For Al the same maximum concentrations could have been reached than for InP if simulations with lower values of τ would have been performed.

In the experimental study Ga^+/Cs° bombardment on GaAs and Ni samples induced surface roughness on the bottom of the crater which was too important to evaluate the crater volume and made subsequent useful yield calculations impossible. So Ga^+/Cs° bombardment on these targets has not been simulated.

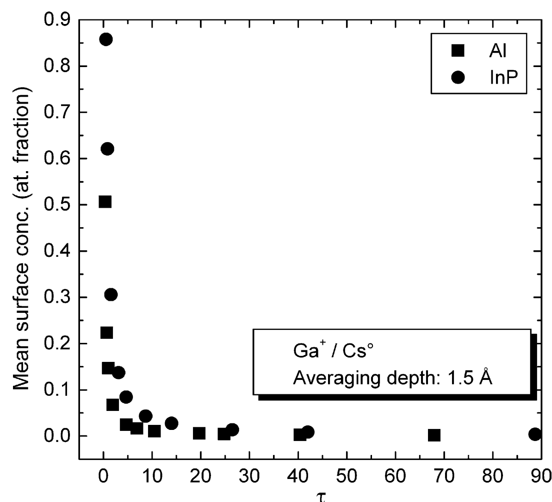

Fig. 5. Mean surface concentration for Ga^+/Cs° bombardment on Al and InP with respect to τ.

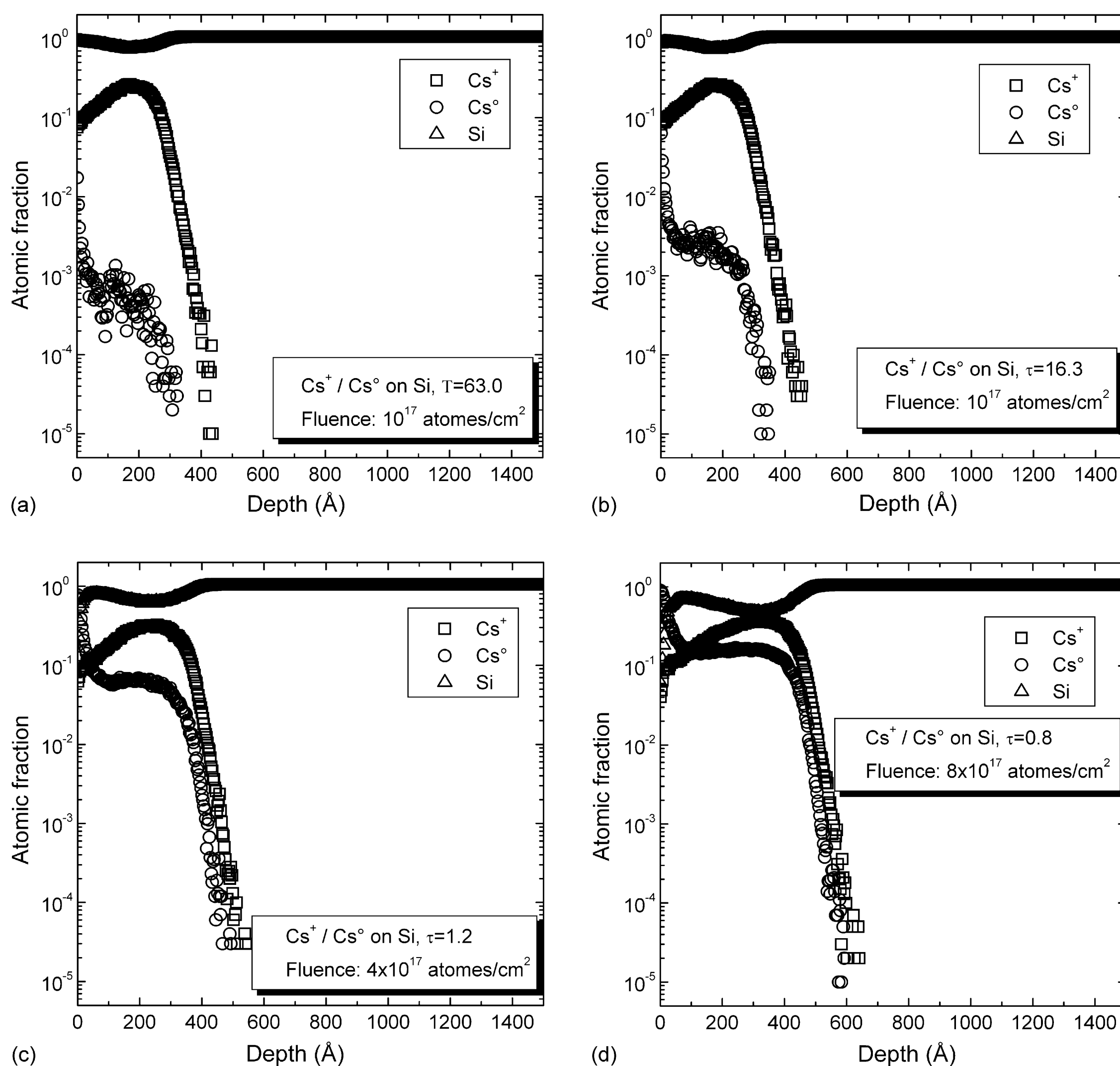

Fig. 6. Depth profiles of Cs^+, Cs° and Si for Cs^+/Cs° bombardment on Si: (a) $\tau = 63.0$, (b) $\tau = 16.3$, (c) $\tau = 1.2$ and (d) $\tau = 0.8$.

3.2. Simulations for Cs^+/Cs° bombardment

During the experiments in the previous study, the maximum analysis sensitivity could not be achieved by Ga^+/Cs° bombardment. Cs^+/Cs° bombardment was expected to produce higher Cs surface concentrations, which could not be observed [27]. Cs^+/Cs° simulations are used to confirm this observation and to identify the influence of the primary ion type on the Cs surface concentration when comparing the results to the simulations for Ga^+/Cs° bombardment.

Once more, only the results for Cs^+/Cs° bombardment on Si will be presented in detail. Fig. 6 shows implantation profiles in the equilibrium regime of Cs^+, Cs° and Si for different values of T (63.0, 16.3, 1.2 and 0.8). Similarly to Fig. 1, the sign $^+$ indicates the primary ion, the sign$^\circ$ neutral Cs deposited at the sample surface and no sign is used for the elements of the sample. For T equal to 63.0 or 16.3 a fluence of 10^{17} atoms/cm^2 is sufficient to reach the equilibrium regime. For T equal to 1.2 or 0.8 a fluence of 4×10^{17} atoms/cm^2, respectively a fluence of 8×10^{17} atoms/cm^2, is necessary to arrive at the equilibrium regime. In contrast to Ga^+/Cs° bombardment, there is always a minimum Cs atomic fraction of 0.1 induced by implantation of Cs^+ primary ions. The Cs atomic fraction due to neutral Cs° deposition is equal to the Cs^+ atomic fraction for a value of T equal to 16.3 and increases up to 1 for lower values of T ($T = 0.8$). The shape of implanted Cs° atoms produced by Cs^+/Cs° bombardment is identical to the Ga^+/Cs° bombardment.

The variation of the total Cs concentration (Cs^+ concentration and Cs° concentration) with respect to the depth and to the fluence is shown in Fig. 7 for a value of T equal to 1.2. Even for a small fluence (8.0×10^{15} atoms/cm^2) the Cs surface concentration due to Cs° deposition is almost maximal whereas the concentration of Cs due to implanted Cs^+ ions reaches equilibrium only for a fluence of about 3.2×10^{17} atoms/cm^2. In addition, fluctuations of the maximal Cs concentration with respect to the fluence are much smaller than for Ga^+/Cs° bombardment.

The Cs^+ primary ion surface concentration does not depend on the parameter T. Increasing Cs° surface concentration lower

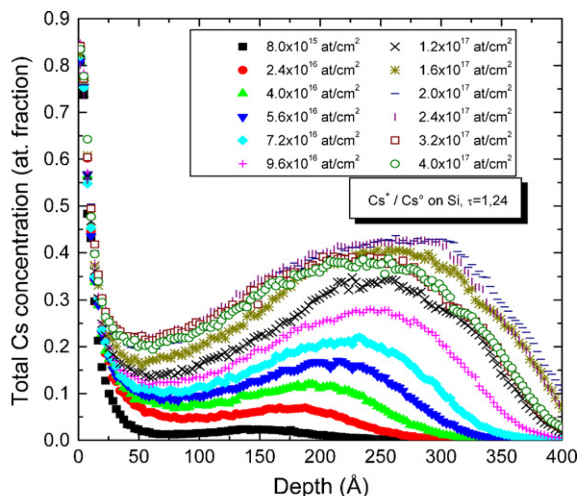

Fig. 7. Total Cs concentration (sum of Cs^+ concentration and Cs° concentration) with respect to the depth for $\tau = 1.2$ (Cs^+/Cs° bombardment on Si). The fluence is varying between 8.0×10^{15} and 4.0×10^{17} atoms/cm^2.

the Si surface concentration. This behaviour was also observed for Ga^+/Cs° bombardment.

The mean Cs surface concentrations (sum of Cs^+ and Cs° concentrations) averaged over different depths have been calculated from the simulated data and plotted with respect to parameter T (Fig. 8). Again, the depths indicated in the graph caption represent the depth over which the concentrations have been averaged. The overall behaviour is identical to Ga^+/Cs° bombardment (Fig. 3). The mean surface concentrations decrease steeply for low values of T. For higher values of T they become close to 0.1 which is the concentration due to the implantation of Cs^+ ions. The influence of the depth over which the concentrations have been averaged becomes apparent for T smaller than 18. For the smallest value of T the concentration averaged over 1.5 Å is almost twice as large than the concentration averaged over 49.5 Å.

For the same reasons than for the Ga^+/Cs° bombardment, the surface concentrations averaged over a depth over 1.5 Å will be used to compare the simulation results to the experimental study.

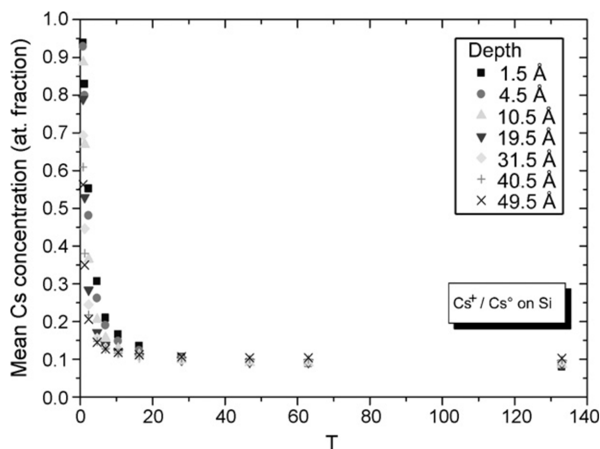

Fig. 8. Mean Cs surface concentration (by considering Cs^+ ions and Cs° atoms) with respect to T calculated by averaging the concentration evolution over depths varying from 1.5 to 49.5 Å (Cs^+/Cs° bombardment on Si).

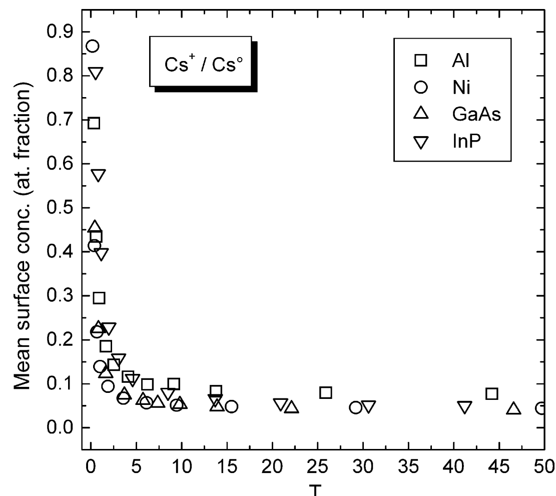

Fig. 9. Mean surface concentration for Cs^+/Cs° bombardment on Al, Ni, GaAs and InP with respect to τ.

Simulation results for Cs^+/Cs° bombardment on Al, Ni, GaAs and InP show a similar behaviour than the simulations on Si, allowing presenting only the mean surface concentrations averaged over a depth of 1.5 Å (Fig. 9). Al presents slightly higher Cs surface concentrations than the other targets (which show all similar concentrations) for high values of T. Al (26.9 amu) is the lightest atom when compared to Ni (58.7 amu), Ga (69.7 amu), As (74.9 amu), In (114.8) and P (30.9 amu). On all targets, Cs^+/Cs° bombardment induces a steep increase of the Cs surface concentration for T smaller than 5.

4. Discussion

In the TRIDYN simulations, the treatment of the surface binding energy, which is only used as a sputtering moderator, is quite delicate. In such simulation codes that use the binary collision approximation with purely repulsive potentials, adjusting the surface binding energy to the heat of sublimation becomes problematic when mixing takes place at the sample surface. In particular, it has been shown that these settings seem to lead to too low Cs surface concentrations for Cs bombardment on Si [38]. Definite conclusions were not possible as thermodynamic effects are not considered in this simulation model. The simulations described in this paper differ from the later ones as ion bombardment with simultaneous neutral Cs deposition is used. For Cs^+ bombardment on a target, the Cs surface concentration is determined by the sputtering of implanted Cs^+ ions, whereas for other ion bombardment with simultaneous Cs° deposition the Cs surface concentration is mainly defined by the deposited Cs atoms and to a lesser degree by the sputtering of implanted Cs° atoms. Still, the simulated Cs surface concentrations are probably systematically lower than the experimental concentrations that could not have been determined [27].

A second point which influences the Cs surface concentration is the sticking of deposited Cs on the sample surface. Whereas Cs adsorbs easily on other surfaces, the sticking coefficient of Cs on itself is low limiting Cs adsorption on most substrates to one monolayer [12,39,40]. This implies that for high Cs deposition

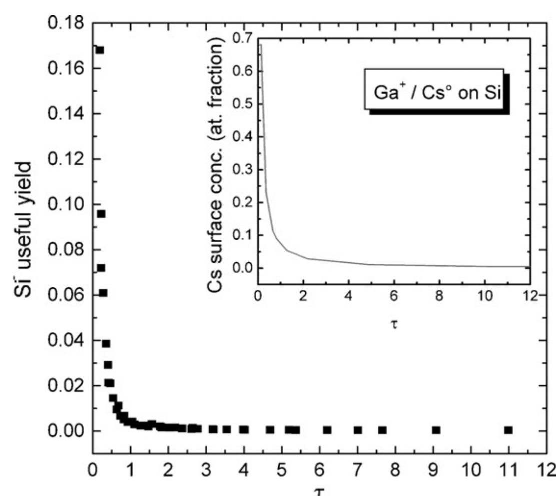

Fig. 10. Comparison of Si^- useful yield variation and Cs surface concentration evolution with respect to τ for Ga^+/Cs° bombardment.

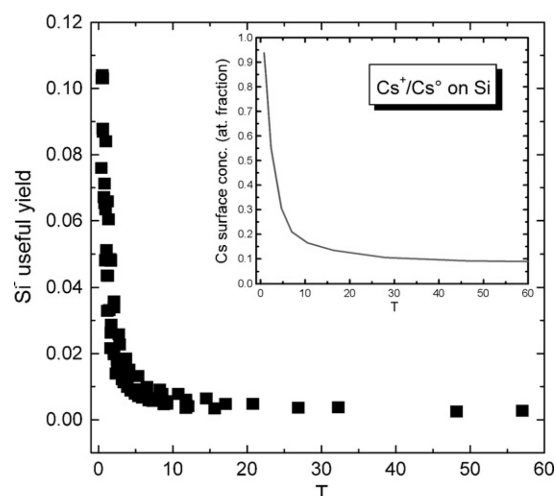

Fig. 11. Comparison of Si^- useful yield variation and Cs surface concentration evolution with respect to T for Cs^+/Cs° bombardment.

rates during the experiments only a part of the incident Cs° atoms sticks on the surface and contributes to the sensitivity increase in SIMS analysis, while in the simulations all incident Cs° atoms stick on the surface producing a Cs surface concentration larger than the experimental concentration.

Thus, the simulated Cs surface concentration is influenced by two processes: it is decreased by adjusting the surface binding energy to the heat of sublimation and increased by the sticking of all Cs atoms on the surface for a coverage close to the monolayer, i.e., for very small values of τ or T. These considerations have to be taken into account when comparing the experimental analysis sensitivities to the simulated Cs surface concentrations. Besides, maximum Cs surface concentrations for the different targets and bombardment conditions cannot be compared because they depend on primary ion type, target composition and simulation conditions. As the concentration varies very rapidly with respect to small values of τ and T, only a large number of simulations exploring the range of small values of τ and T methodically can produce identical maximum Cs surface concentrations. Nevertheless, these precautions do not take into account the surface binding energy adjusted to the heat of sublimation whose consequences will probably depend on the nature of the target.

The simulated Cs surface concentrations are compared to the variation of the analysis sensitivity of the previous study [27]. The analysis sensitivity has been described by the useful yield which has been defined by:

$$\mathrm{UY}(\mathrm{M}^-) = \frac{\text{number of detected } \mathrm{M}^- \text{ ions}}{\text{number of sputtered M atoms}} \tag{3}$$

In Figs. 10 and 11, the Si^- useful yield and the Cs surface concentration have been plotted for Ga^+/Cs° bombardment, respectively for Cs^+/Cs° bombardment, with respect to the parameter τ or T. The simulated data shows the mean Cs surface concentration averaged over a depth of 1.5 Å. For both bombardment conditions, the Cs surface concentration is almost constant for high values of τ or T. The same behaviour is observed for the Si^- useful yields. Towards smaller values of τ or T, the Cs surface concentration and the Si^- useful yield increase steeply as well for Ga^+/Cs° bombardment as for Cs^+/Cs° bombardment. The correlation between Cs concentration and useful yield agrees qualitatively with the electron-tunneling model describing ion emission from semi-conducting and metallic surfaces:

$$\begin{cases} \beta_{\mathrm{M}}^- = 1 & \text{if } \phi < A \\ \beta_{\mathrm{M}}^- \propto \mathrm{e}^{-\frac{(\phi - A)}{\varepsilon n}} & \text{if } \phi > A \end{cases} \tag{4}$$

where β_{M}^- is the secondary ion ionization probability, Φ the work function of the sample and A is the electron affinity of the sputtered atom. The deposited Cs atoms decrease the sample work function. The secondary ion ionization probability and thus the useful yield, which is proportional to the ionization probability, vary exponentially with the sample work function. So, increasing Cs surface concentrations should induce rising useful yields. This prediction is verified in Figs. 10 and 11. The other targets (Al and InP for Ga^+/Cs° bombardment and Al, Ni, GaAs and InP for Cs^+/Cs° bombardment) exhibit the same correlation between Cs surface concentration and useful yield.

The experimental and simulation results are used to plot the useful yields with respect to the simulated Cs surface concentrations in order to visualize the dependence of the useful yields on the Cs surface concentrations and to verify the quality of experimental and simulated results (Figs. 12 and 13). In Fig. 12 (Ga^+/Cs° bombardment), the useful yields of all analyzed ions (Si^-, Al^-, P^- and In^-) increase very steeply for small Cs surface concentrations. The almost vertical useful yield variations are probably due to the adjustment of the surface binding energy to the heat of sublimation producing too low Cs concentrations at high values of τ and T and to a lesser degree to an experimental uncertainty in the determination of τ and T. For Si the useful yield shows a moderate increase at higher values of τ, but constant values are not attained indicating that the sample work function can apparently not be lowered below the electron affinity of the analyzed element (necessary for quantification in SIMS) [27]. The Al target reveals a similar variation of the useful yield with respect to the Cs surface concentration for higher Cs concentra-

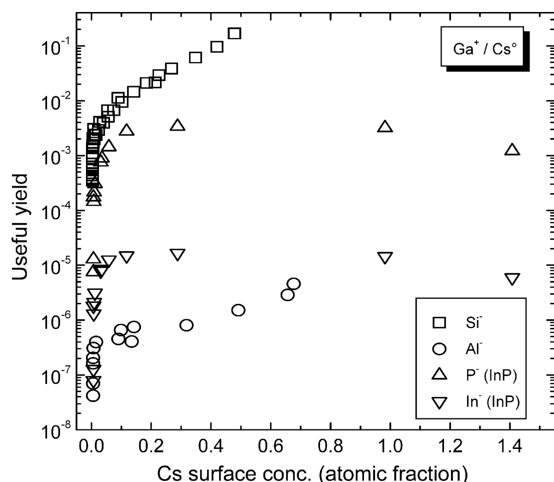

Fig. 12. Useful yields of Si^-, Al^-, P^- and In^- with respect to the Cs surface concentration for Ga^+/Cs° bombardment.

tion, except that the growth is less pronounced. The useful yields of P^- and In^- are constant for higher Cs surface concentrations. As these useful yields remain lower than the transmission of the instruments (≈20%) [20], total ionization is not attained. The electron work function cannot be lowered sufficiently, making higher useful yields impossible. Maximum useful yields depend on sample work function and electron affinity of the analyzed element. In addition, Cs surface concentrations (atomic fraction) larger than 1 are observed for this target. Concentrations larger than 1 are due to the extrapolation at low τ (respectively T) values in the Cs surface concentration versus τ (respectively T) plot. This artefact is due to the problems concerning surface binding energy and sticking factor mentioned above. During the experiments Cs exhibits a poor sticking coefficient for concentrations close to the monolayer and during the simulations all incident Cs atoms stick on the surface (independent of Cs surface concentration), providing simulated Cs surface concentrations larger than the experimental concentrations.

The useful yields with respect to the Cs surface concentration for Cs^+/Cs° bombardment behave similarly (Fig. 13). For very small Cs concentrations, the useful yields increase almost vertically, the reason being the same than for Ga^+/Cs° bombardment. At higher Cs concentrations, the variations of the Si^-, Al^-, P^- and In^- useful yields are identical to Fig. 12. The Ni^- useful yield increases to constant values which are quite close to the maximum sensitivity on the CMS [27]. As^- and Ga^- useful yields increase also to a plateau, except that the maximum useful yields remain lower indicating that no additional lowering of the sample work function is possible. Once more, simulated Cs surface concentrations larger than 1 are due to the difference of Cs sticking in experiments and simulations.

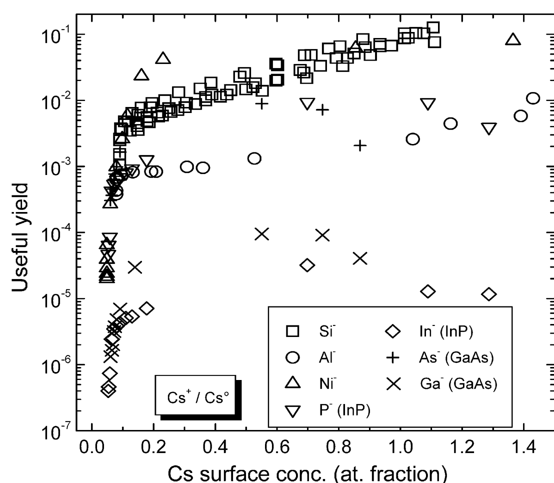

Fig. 13. Useful yields of Si^-, Al^-, Ni^-, P^-, In^-, As^- and Ga^- with respect to the Cs surface concentration for Cs^+/Cs° bombardment.

5. Conclusions

In a previous study, the SIMS analysis sensitivity of negative secondary ions has been studied on various samples (analyzed elements) for two types of primary ion bombardment and simultaneous neutral Cs deposition. During these studies, experimental conditions were varied in order to get different Cs surface concentrations and thus increased secondary ion sensitivities. As the Cs concentration could not be determined experimentally, the TRIDYN code has been used in this paper to simulate this concentration for the different experimental conditions. The TRIDYN code gives implantation profiles as well as the sputtering yields of the implied elements with respect to the primary ion fluence. The implantation profiles in steady state conditions have been used to calculate mean Cs surface concentrations by averaging over different depths and taking the averaging depth presenting the highest Cs concentrations. By extrapolation, the secondary ion sensitivities, initially plotted with respect to experimental conditions, have been plotted with respect to the mean Cs surface concentration. In this way a comparison between the electron-tunneling model, used to describe ion emission from metallic and semi-conducting surfaces, and the experimental and simulation results becomes possible. However, the comparison has to be considered with care, because the simulated Cs surface concentration is altered by two artefacts introduced by the simulation model. Fixing the surface binding energy to the heat of sublimation leads to lower Cs surface concentrations whereas the sticking of the cesium in the simulations conducts to increased concentrations compared to experimental values. Nevertheless, the increase of secondary ion sensitivities observed experimentally can be assigned to the increase of the Cs surface concentration. For small Cs concentrations a steep increase of secondary ion sensitivities is observed while almost constant sensitivity values are observed for higher Cs surface concentrations. Final conclusions regarding the useful yield variations with respect to the Cs deposition can only be drawn after measuring the work function shift experimentally, giving experimental evidence for the influence of Cs deposition on ionization processes.

Acknowledgements

This work has been supported by the “Ministère de la Culture, de l’Enseignement Supérieur et de la Recherche” of Luxembourg.

References

[1] M.G. Dowsett, R.D. Barlow, Anal. Chim. Acta 297 (1994) 253.
[2] P.C. Zalm, Rep. Prog. Phys. 58 (1995) 1321.
[3] G. Stingeder, Anal. Chim. Acta 297 (1994) 231.
[4] J.-N. Audinot, S. Schneider, M. Yegles, P. Hallegot, R. Wennig, H.-N. Migeon, Appl. Surf. Sci. 231–232 (2004) 490.
[5] R. Levi-Setti, K.L. Gavrilov, P.L. Strissel, R. Strick, Appl. Surf. Sci. 231–232 (2004) 479.
[6] S. Chandra, Appl. Surf. Sci. 231–232 (2004) 462.
[7] H.A. Storms, K.F. Brown, J.D. Stein, Anal. Chem. 49 (1977) 2023.
[8] M.A. Karolewski, R.G. Cavell, Appl. Surf. Sci 193 (2002) 11.
[9] K. Wittmaack, Surf. Sci. 126 (1983) 573.
[10] M. Scheffler, C. Stampfl, Theory of adsorption on metal substrates, in: K. Horn, M. Scheffler (Eds.), Handbook of Surface Science, Vol. 2: Electronic Structure, Elsevier, Amsterdam, 2000, pp. 286–356.
[11] A. Hohlfeld, M. Sunjic, K. Horn, J. Vac. Sci. Technol. A 5 (4) (1987) 679.
[12] B. Kierren, D. Paget, J. Vac. Sci. Technol. A 15 (4) (1997) 2074.
[13] D. Heskett, T. Maeda, A.J. Smith, W.R. Graham, N.J. DiNardo, E.W. Plummer, J. Vac. Sci. Technol. B 7 (4) (1989) 915.
[14] P. Soukiassian, L. Spiess, K.M. Schirm, P.S. Mangat, J.A. Kubby, S.P. Tang, A.J. Freeman, J. Vac. Sci. Technol. B 11 (4) (1993) 1431.
[15] H. Gnaser, Phys. Rev. B 54 (23) (1996) 16456.
[16] T. Kan, K. Mitsukawa, T. Ueyama, M. Takada, T. Yasue, T. Koshikawa, J. Surf. Anal. 5 (1) (1999) 52.
[17] P.A.W. van der Heide, Appl. Surf. Sci. 157 (2000) 191.
[18] H. Gnaser, Phys. Rev. B 63 (2001) 45425.
[19] P.A.W. van der Heide, Nucl. Instrum. Meth. Phys. Res. B 194 (2002) 489.
[20] T. Mootz, B. Rasser, P. Sudraud, E. Niehuis, T. Wirtz, W. Bieck, H.-N. Migeon, in: A. Benninghoven, P. Bertrand, H.-N. Migeon, H.W. Werner (Eds.), Secondary Ion Mass Spectrometry SIMS XII, Elsevier, Amsterdam, 2000, p. 233.
[21] T. Wirtz, B. Duez, H.-N. Migeon, H. Scherrer, Int. J. Mass Spectrom. 209 (2001) 57.
[22] P. Philipp, T. Wirtz, H.-N. Migeon, H. Scherrer, Appl. Surf. Sci. 231–232 (2004) 754.
[23] T. Wirtz, H.-N. Migeon, H. Scherrer, Int. J. Mass Spectrom. 225 (2003) 135.
[24] T. Wirtz, H.-N. Migeon, Surf. Sci. 557 (2004) 57.
[25] T. Wirtz, H.-N. Migeon, Surf. Sci. 561 (2004) 200.
[26] T. Wirtz, H.-N. Migeon, Appl. Surf. Sci. 231–232 (2004) 940.
[27] P. Philipp, T. Wirtz, H.-N. Migeon, H. Scherrer, Int. J. Mass Spectrom 253 (2006) 71–78.
[28] H. Oechsner, Anal. Chim. Acta 283 (1993) 131–138.
[29] W. Bock, H. Gnaser, H. Oechsner, Anal. Chim. Acta 297 (1994) 277–283.
[30] H. Gnaser, W. Bock, H. Oechsner, Appl. Surf. Sci. 70/71 (1993) 44–48.
[31] W. Möller, W. Eckstein, Nucl. Instrum. Meth. Phys. Res. B 2 (1984) 814.
[32] W. Möller, W. Eckstein, J.P. Biersack, Comput. Phys. Commun. 51 (1988) 355.
[33] W. Eckstein, J.P. Biersack, Appl. Phys. A 37 (1985) 95.
[34] J.P. Biersack, L.G. Haggmark, Nucl. Instrum. Meth. 174 (1980) 257.
[35] J.P. Biersack, W. Eckstein, Appl. Phys. A 34 (1984) 73.
[36] W. Eckstein, W. Möller, Nucl. Instrum. Meth. Phys. Res. B 7/8 (1985) 727.
[37] TRIDYN_FZR Manual, http://www.fz-rossendorf.de.
[38] W. Eckstein, M. Hou, V.I. Shulga, Nucl. Instrum. Meth. Phys. Res. B 119 (1996) 477.
[39] C.I. Wu, A. Kahn, Appl. Phys. Lett. 74 (10) (1999) 1433.
[40] J.E. Ortega, R. Miranda, Appl. Surf. Sci. 56–58 (1992) 211.